

Carrier-Envelope Phase Controlling of Ion Momentum Distributions in Strong Field Double Ionization of Methyl Iodide

Published as part of *The Journal of Physical Chemistry virtual special issue "Paul L. Houston Festschrift"*.

Gabriel Stewart, Duke Debrah, Paul Hoerner, Suk Kyoung Lee, H. Bernhard Schlegel, and Wen Li*



Cite This: <https://doi.org/10.1021/acs.jpca.2c06754>



Read Online

ACCESS |



Metrics & More

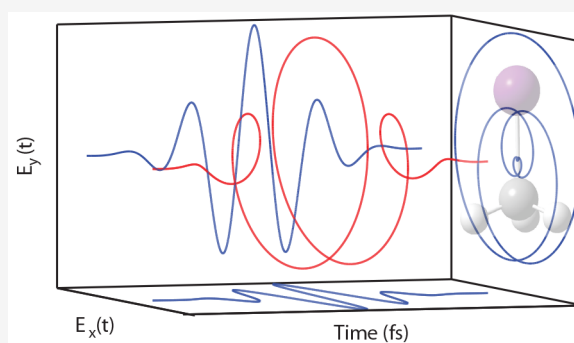


Article Recommendations



Supporting Information

ABSTRACT: In strong field ionization of methyl iodide initiated by elliptically polarized few-cycle pulses, a significant correlation was observed between the carrier-envelope phases (CEPs) of the laser and the preferred ejection direction of methyl cation arising from dissociative double ionization. This was attributed to the carrier-envelope phase dependent double ionization yields of methyl iodide. This observation provides a new way for monitoring the absolute CEPs of few-cycle pulses by observing the ion momentum distributions.



INTRODUCTION

The possibility of driving and manipulating photoinduced chemical reactions has been extensively explored in the past decades. Controlling the product momentum distributions arising from photodissociation is one aspect of laser control. In the weak field regime, the product momentum distributions are determined by the relationship between the transition dipoles and the driving laser electric field.^{1,2} In contrast, because strong field ionization involves many transitions and many photons, the product momentum distributions do not directly correlate with any particular transition dipole. As a result, the ionization rates and thus the product momentum distributions depend on the laser electric field and the shape of the ionizing orbitals.^{3–9} Therefore, parametrization of the laser is crucial for steering the ejection direction of electrons and fragmented molecules.

For ultrashort few-cycle pulses, an important parameter to consider for achieving control is the carrier-envelope phase (CEP). The CEP describes the phase shift between the peak of the envelope function and the peak of the carrier wave. The electric field of an ultrashort pulse can be expressed as $E(t) = E_0 e^{-(t/\tau)^2} \cos(\omega t + \theta)$, in which E_0 is the envelope function, ω is the angular frequency, τ is the pulse duration, and θ is the carrier-envelope phase. For ultrafast studies, the CEP is important because it determines the temporal evolution of an ultrashort pulse while it is less significant in long pulses. This becomes critically important in high harmonic generation,^{10,11} nonsequential ionization,¹² and control over photochemical reactions.¹³

Various methods have been developed and applied to measure the CEP. Although, it should be noted that these

techniques only measure the relative CEP rather than the absolute CEP of ultrashort pulses. The f -to- $2f$ interferometry is a well-established self-referencing method,^{14–16} that measures the interference between the short wavelength part of fundamental spectrum and the long wavelength part of the frequency doubled spectrum. Alternatively, the above threshold ionization (ATI) phasemeter is a popular CEP measurement technique developed by Paulus and co-workers.^{17,18} This approach utilizes linearly polarized light to measure the asymmetric momentum distributions of photoionized electrons to obtain the CEP. However, theoretical calculations are always necessary for retrieving the CEP offset.

Recently, Li and co-workers developed an *in situ* method for directly measuring the absolute CEP with strong field ionized electrons using a velocity map imaging setup.¹⁹ This technique measures the angle of maximum ionization which corresponds to the peak of the electric field. The peak of the electric field directly coincides with the CEP for circularly polarized light.²⁰ The study showed that the absolute CEP of a pulse could be directly measured without theory input. However, complications arising from population depletion and a finite deflection angle due to the interaction between departing electrons and the cores can affect its accuracy.²¹

Received: September 22, 2022

Revised: January 4, 2023

One potential method to circumvent these issues is to use ejected ions to measure the CEP, if such a correlation exists. The rationale behind this is that ejection angles of ions are not subject to deflection experienced by electrons because of the substantial mass of the ions. Using the CEP to control the ion ejection direction has been realized in previous studies using linearly polarized light.^{22–26} It has not been explored with circularly or elliptically polarized light.

In this work, we demonstrate that the ion imaging technique can be utilized to acquire the 2D momentum distribution of dissociated ions in the plane of polarization to determine the CEP of circularly/elliptically polarized light. From these results, we found the ion ejection direction strongly correlates with the CEPs of ultrashort pulses. Furthermore, our theoretical modeling suggests that the absolute CEPs can be directly obtained from the preferred ejection direction of ions.

METHODS

The experimental setup has been described in detail in previous studies.^{19,27–32} Here, we will briefly discuss the major components involved in this experiment and modifications that were made to the original configuration. Pulses from a 1 kHz Ti:sapphire two-stage amplified laser (KMLabs Red Dragon, 800 nm, 30 fs, 1 mJ/pulse) were spectrally broadened using a 1 m long hollow-core fiber (Imperial Consultants (ICON) of Imperial College London) filled with argon gas. Seven pairs of chirped mirrors (Ultrafast Innovation, PC70) coupled with a pair of BK7 wedges were used to compress the pulse. A D-scan technique³³ was used to fully characterize the pulse and retrieved a duration of ~ 5 fs.

A broadband quarter-wave plate (United Crystals, AWP650-1100) was used to produce elliptically polarized light (0.9 ellipticity) that was directed into a VMI detection system. CH₃I (Sigma-Aldrich, 99%) was bubbled into the gas line with helium as the carrier gas. With a skimmer, a supersonically expanded cold molecular beam was used to introduce the samples into the main chamber. The electron/ion electrodes were pulsed to accelerate both ions and electrons toward the detector. A microchannel plate/phosphor screen (MCP) imaging detector coupled with two complementary metal-oxide-semiconductor (CMOS) cameras was utilized to acquire the 2D angular distributions of photoionized events. The cameras were run at 1 kHz and synchronized with the laser trigger. Their exposure times were adjusted to collect only ions or electrons,³⁴ respectively.

A unique feature of the setup is the laser detector configuration. The laser beam was pointed toward the detector directly but was intercepted by a focusing mirror ($f = 100$ mm) placed directly in front of the MCP detector, within the main chamber.¹⁹ The laser beam was then focused back onto the molecular beam to produce ionization/dissociation events. With this configuration, the 2D images obtained were direct measurements of the momentum of ions and electrons in the plane of polarization. Conventionally, the laser beam is parallel to the detector and momenta in the plane of polarization can only be achieved through 3D measurements, which has limited count rate due to a finite detector deadtime.

Finally, a camera-based f -to- $2f$ setup was also employed concurrently with the VMI technique to monitor the relative CEP of each laser pulse.^{19,35–37} Because the laser system is not phase-stabilized, the f -to- $2f$ is necessary for tagging the relative CEP of each pulse to provide a reference for each camera images.

Theoretically, time-dependent configuration interaction with a complex absorbing potential (TDCI-CAP) was used in simulations of strong field ionization to model the CEP dependence of CH₃I double ionization.³⁸ Because the pulse is close-to-circularly polarized, electron recollision is suppressed and thus double ionization proceeds by a sequential process (CH₃I \rightarrow CH₃I⁺ + e ; CH₃I⁺ \rightarrow CH₃I²⁺ + e). Sequential double ionization was modeled by two independent TDCI simulations. Details of the TDCI methodology are described in the Supporting Information. The first simulation uses time-dependent configuration interaction with single excitations (TD-CIS) and yields the population of the cation, $|\Psi_{\text{cation}}^a(t)|^2$, produced from the neutral from the beginning of the pulse, t_0 , to time t , starting from a unit population of the neutral at time t_0 .

$$|\Psi_{\text{cation}}^a(t)|^2 = 1 - |\Psi_{\text{neutral}}^a(t)|^2 \quad (1)$$

The second simulation for ionization of the cation uses time-dependent configuration interaction including single and double excitations with ionization (TD-CISD-IP) and yields the amount of dication, $|\Psi_{\text{dication}}^b(t)|^2$, produced from the cation from time t to the end of the pulse, t_1 , starting from a unit population of the cation at time t .

$$|\Psi_{\text{dication}}^b(t)|^2 = (|\Psi_{\text{cation}}^b(t)|^2 - |\Psi_{\text{cation}}^b(t_1)|^2) / |\Psi_{\text{cation}}^b(t)|^2 \quad (2)$$

The total amount of dication produced by the pulse is obtained by multiplying eq 2 by eq 1 and integrating over the duration of the pulse from t_0 to t_1 .

$$\text{dication yield} = \int_{t_0}^{t_1} |\Psi_{\text{cation}}^a(t)|^2 |\Psi_{\text{dication}}^b(t)|^2 dt \quad (3)$$

Calculations were carried out with laser pulses with different CEPs for CH₃I molecules fixed in space and the dication yields can be compared with experimental results. This is because the majority of dications will eventually dissociate.⁷ We also note the sequential ionization simulations were performed with a fixed nuclear geometry of the ground state neutrals. This is justified by the fact that most of the ionization takes place around the peak of the laser envelope due to the strong nonlinearity of SFI (see Supplemental Figure S2). The ~ 5 fs pulse duration ensures nuclear motion during the pulse to be minimal.

RESULTS AND DISCUSSION

Two factors are important to consider when selecting appropriate molecular systems in this study: (1) The angle dependent ionization rate of the molecules must be anisotropic. (2) The dissociation of the molecule must be faster than the rotation period. The first condition can be easily satisfied by a molecule without inversion symmetry. Inversion symmetry prevents distinguishing between 0 and 180°. A fast dissociation ensures that the molecular axis at the moment of ionization is maintained so that the ion ejection direction gives the molecular orientation. This is the axial recoil approximation. By satisfying these two conditions, the ion momentum distributions can map out the angle-dependent ionization rates and thus provide information on the CEPs of the driving laser pulses. In this study, CH₃I was selected because it fulfills both requirements.^{7,39,40}

The experimental results of CEP resolved methyl cation momentum distribution are shown in Figure 1. The dark

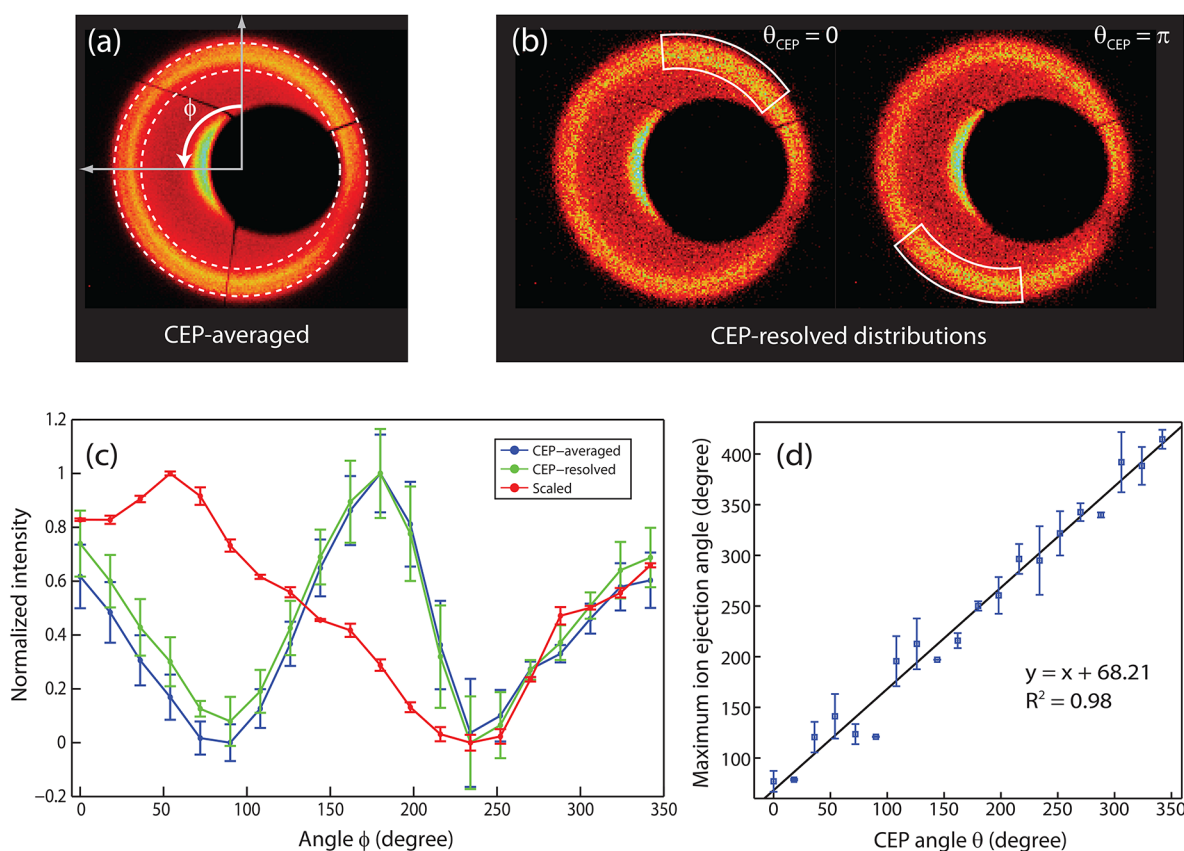


Figure 1. (a) CEP averaged CH_3^+ momentum distribution in the plane of polarization. The signal between the two dashed circles was integrated to give the angle dependent yields in Figure 1c. (b) CEP-resolved CH_3^+ momentum distribution at different CEP values 0 and π (relative), respectively. The white contour lines are highlighting the regions of the highest yield of CH_3^+ for a given CEP, 0 or π respectively. Note the CEP is relative as measured by the f -to- $2f$ method. (c) Scaling the angular distribution of a CEP resolved methyl cation momentum (green) with that of CEP averaged cation (blue) to retrieve the CEP (red). Note all curves were normalized according to $\frac{Y - Y_{\min}}{Y_{\max} - Y_{\min}}$. (d) Correlation plot between the maximum ion ejection angle and the CEP given by the f -to- $2f$. With a slope = 1, the fitted trendline shows the strong correlation between the maximum ion ejection direction and the CEP of the laser. The R^2 value (0.98) indicates the goodness of the linear fitting.

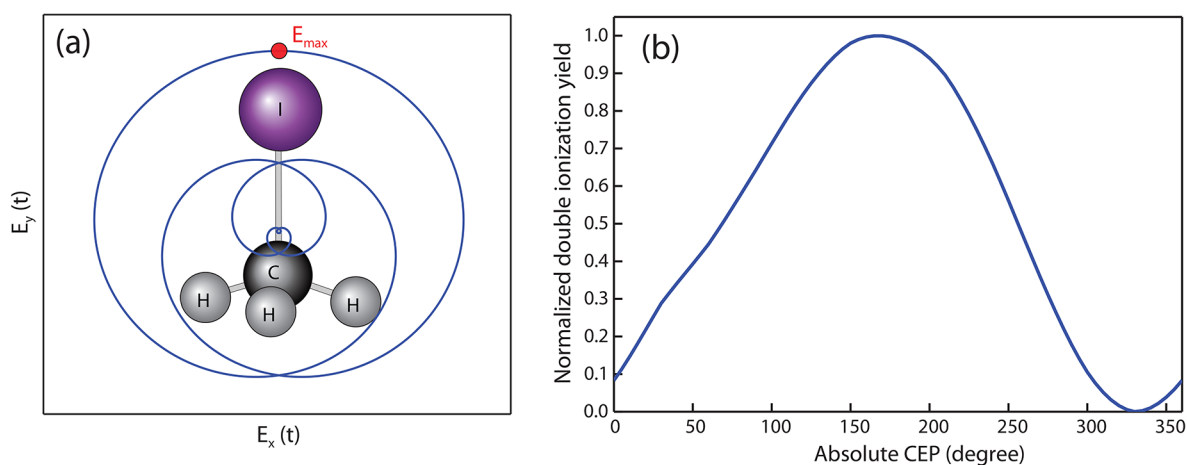


Figure 2. (a) The time evolution of the electric field of a 4-cycle (full width) laser pulse with an absolute CEP of zero. The maximum electric field is pointing up. In the calculation, the C–I bond is fixed in space with the iodine atom at the top. (b) The calculated dication yields at different absolute CEP values.

feature in the center is due to the focusing mirror. No inverse Abel transform was applied to the images because these images do not possess cylindrical symmetry. Here we focus our attention on the outmost feature, which arises from the dissociation of doubly ionized methyl iodide. Dissociative

single ionization can also take place, but the resulting methyl cation has much smaller kinetic energy and is masked by the focusing mirror. Figure 1a plots the images of methyl cation with all CEPs included. For circularly polarized light, the angular distribution should be isotropic. However, the

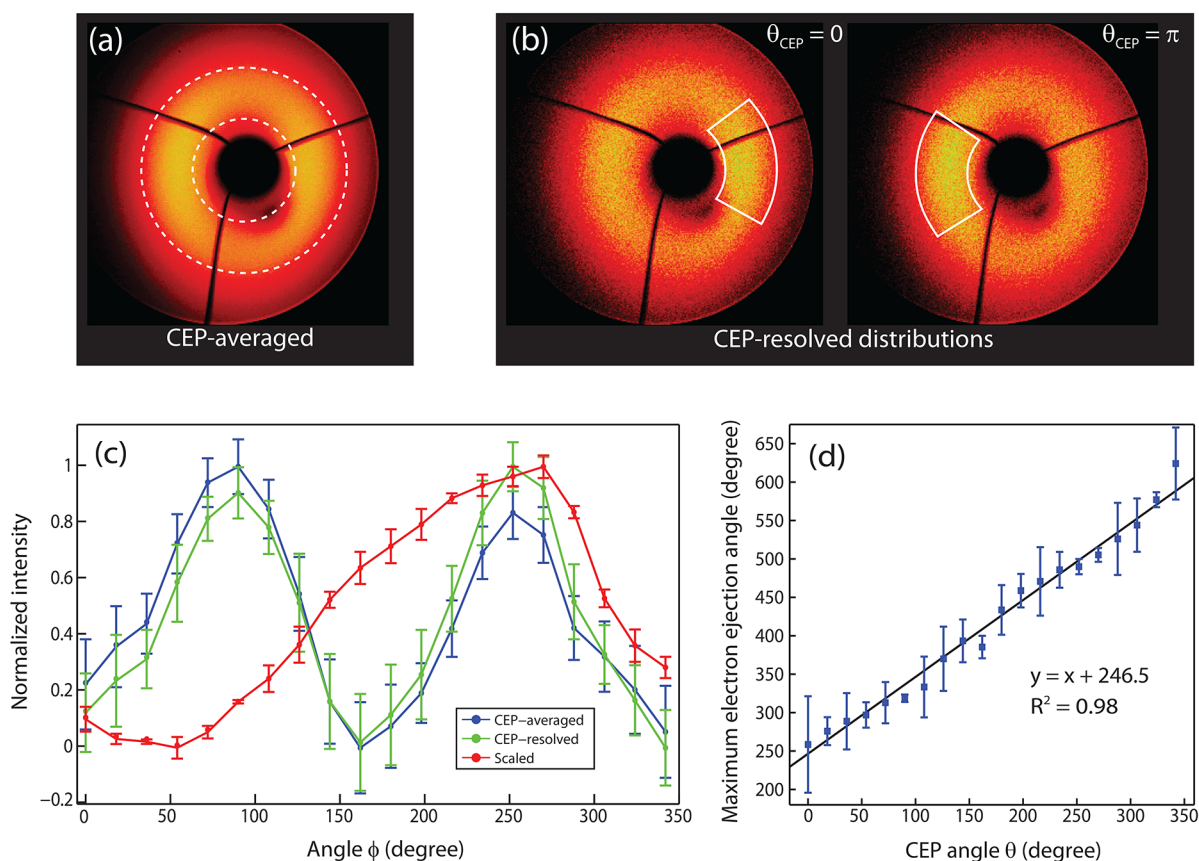


Figure 3. Same method as in Figure 1 but applied to electrons. (a) CEP averaged electron momentum distribution in the plane of polarization. The signal between the two dashed circles was integrated to give the angle dependent yields in Figure 3c. These are designated as slow electrons. (b) CEP-resolved electron momentum distributions at different relative CEP values 0 and π , respectively. The white contour lines are highlighting the regions of the highest density of detected electrons for a given CEP. (c) Scaling the angular distribution of a CEP resolved electron momentum (green) with that of CEP averaged electrons (blue) to retrieve the CEP (red). Note all curves were normalized according to $\frac{Y - Y_{\min}}{Y_{\max} - Y_{\min}}$. (d) Correlation plot between the maximum electron ejection angle and the CEP given by the f -to- $2f$. With a slope = 1, the fitted trendline shows the strong linear relationship between the maximum electron ejection direction and the CEP of the laser.

distribution observed here is not isotropic due to a nonperfect ellipticity of the laser (0.9) and detector inhomogeneity. Figure 1b shows two CH_3^+ images at two different CEPs. The images show somewhat different momentum distributions. To quantitatively characterize this difference, we adopted a scaling process in which we used the CEP averaged angular distribution (blue curve in Figure 1c) to divide each CEP resolved angular distribution. A sample result is shown in Figure 1c (green and red curves for before and after the scaling, respectively). Note each curve was normalized separately). The scaled curve now shows a clear maximum at a certain angle and this angle changes with the CEP. It turns out this angle is uniquely associated with the CEP. This can be seen from Figure 1d, in which we plot the maximum ejection angle of ion at each CEP value. A strong linear relationship is observed and the slope of 1 is a clear indication of the correlation between the ion ejection angle and the CEP value.

While the correlation is clearly present, the experimental result itself cannot tell the offset between the preferred ion ejection direction and the absolute CEP value, i.e., the question of whether the preferred ion ejection gives the direction of the maximum electric field of the pulse. This is because the CEP values obtained by the f -to- $2f$ method are only relative and thus an arbitrary CEP offset is present. To determine this offset, theoretical modeling is required. Figure 2a shows the electric

field evolution of a laser pulse with an absolute CEP of zero (maximum electric field is pointing up toward iodine atom). As the absolute CEP values are varied, the maximum electric field direction will rotate in the plane of the polarization, which changes the dication yields. Figure 2b shows the calculated total dication yield as a function of the absolute CEP (normalized to a range of 0 to 1). The curve shows a clear maximum, confirming the experimentally observed correlation between the preferred ion ejection direction and CEPs. The maximum is at 167° . This suggests that maximum double ionization is achieved when the absolute CEP is pointing to the methyl group, which is in total agreement with previous recoil-frame angle dependent measurements.⁷ With the axial recoil approximation, this gives a 13° offset between the absolute CEP and the measured preferred CH_3^+ ejection direction.

This result was corroborated by the measurements of electrons. Figure 3 shows the same approach to extract the CEP information from the electron momentum distributions. We note that the maximum ionization direction of electrons strongly depends on the magnitude of the momentum, which is a clear sign of neutral depletion due to a high laser intensity.²¹ However, with slow electrons, the offset between methyl cation and electrons was measured to be $89^\circ \pm 8^\circ$. This was done by taking the difference between the intercepts of the fitted linear equations. This result is from separate coincidence

measurements between electrons and ions with a lower count rate, which was achieved by using a much lower gas pressure. This offset matches almost perfectly with a 90° offset due to the vector potential effect.²⁰ On the other hand, the offset between the methyl cation and high energy electrons is close to 160°, which is likely due to the neutral depletion or complex electronic dynamics. This confirms that the method of using electrons to measure absolute CEPs is subject to various complicating effects and much caution is required.

CONCLUSION

In summary, we identified a strong correlation between the angles of maximum ion ejection and the CEPs of the driving laser pulse in methyl iodide. Theoretical results suggest, after correcting a 13° offset, the absolute CEP can be directly obtained from measuring the momentum distributions of methyl cations arising from double ionization of methyl iodide. As far as we know, this is the first time that such a correlation was demonstrated. In the future, it will be interesting to investigate such an effect in other molecular systems. More importantly, this new method can be used to calibrate the absolute CEPs of ultrashort pulses and to study absolute CEP resolved strong field dynamics.

ASSOCIATED CONTENT

Supporting Information

The Supporting Information is available free of charge at <https://pubs.acs.org/doi/10.1021/acs.jpca.2c06754>.

Detailed computational methods employing TDCI (PDF)

AUTHOR INFORMATION

Corresponding Author

Wen Li – Department of Chemistry, Wayne State University, Detroit, Michigan 48202, United States; orcid.org/0000-0002-3721-4008; Email: wli@chem.wayne.edu

Authors

Gabriel Stewart – Department of Chemistry, Wayne State University, Detroit, Michigan 48202, United States

Duke Debrah – Department of Chemistry, Wayne State University, Detroit, Michigan 48202, United States; orcid.org/0000-0002-1281-3012

Paul Hoerner – Department of Chemistry, Wayne State University, Detroit, Michigan 48202, United States

Suk Kyoung Lee – Department of Chemistry, Wayne State University, Detroit, Michigan 48202, United States

H. Bernhard Schlegel – Department of Chemistry, Wayne State University, Detroit, Michigan 48202, United States; orcid.org/0000-0001-7114-2821

Complete contact information is available at: <https://pubs.acs.org/doi/10.1021/acs.jpca.2c06754>

Notes

The authors declare no competing financial interest.

ACKNOWLEDGMENTS

Research supported by National Science Foundation (NSF), AMO-E program, under Award #2012098 (W. L.) and the U.S. Department of Energy (DOE), Office of Science, Basic Energy Sciences (BES), under Award # DE-SC0020994 (H. B. S.).

REFERENCES

- (1) Schiff, L. *Quantum mechanics*; McGraw-Hill: New York, 1955; pp 267–280.
- (2) Zare, R. N. Photoejection dynamics. *Mol. Photochem.* **1972**, *4*, 1–37.
- (3) Jaron-Becker, A.; Becker, A.; Faisal, F. H. M. Dependence of strong-field photoelectron angular distributions on molecular orientation. *J. Phys. B-At. Mol. Opt. Phys.* **2003**, *36* (21), L375–L380.
- (4) Jaron-Becker, A.; Becker, A.; Faisal, F. H. M. Ionization of N-2, O-2, and linear carbon clusters in a strong laser pulse. *Phys. Rev. A* **2004**, *69* (2), 9.
- (5) Tong, X. M.; Zhao, Z. X.; Lin, C. D. Theory of molecular tunneling ionization. *Phys. Rev. A* **2002**, *66* (3), No. 033402.
- (6) Lin, C. D.; Tong, X. M. Dependence of tunneling ionization and harmonic generation on the structure of molecules by short intense laser pulses. *J. Photochem. Photobiol. A-Chem.* **2006**, *182* (3), 213–219.
- (7) Winney, A. H.; Basnayake, G.; Debrah, D. A.; Lin, Y. F.; Lee, S. K.; Hoerner, P.; Liao, Q.; Schlegel, H. B.; Li, W. Disentangling Strong-Field Multielectron Dynamics with Angular Streaking. *J. Phys. Chem. Lett.* **2018**, *9*, 2539–2545.
- (8) Krause, P.; Schlegel, H. B. Angle-Dependent Ionization of Small Molecules by Time-Dependent Configuration Interaction and an Absorbing Potential. *J. Phys. Chem. Lett.* **2015**, *6* (11), 2140–2146.
- (9) Li, W.; Jaron-Becker, A. A.; Hogle, C. W.; Sharma, V.; Zhou, X.; Becker, A.; Kapteyn, H. C.; Murnane, M. M. Visualizing electron rearrangement in space and time during the transition from a molecule to atoms. *Proc. Natl. Acad. Sci. U. S. A.* **2010**, *107* (47), 20219–20222.
- (10) Ishii, N.; Kaneshima, K.; Kitano, K.; Kanai, T.; Watanabe, S.; Itatani, J. Carrier-envelope phase-dependent high harmonic generation in the water window using few-cycle infrared pulses. *Nat. Commun.* **2014**, *5* (1), 3331.
- (11) Sola, I. J.; Mével, E.; Elouga, L.; Constant, E.; Strelkov, V.; Poletto, L.; Villoresi, P.; Benedetti, E.; Caumes, J. P.; Stagira, S.; Vozzi, C.; Sansone, G.; Nisoli, M. Controlling attosecond electron dynamics by phase-stabilized polarization gating. *Nat. Phys.* **2006**, *2*, 319.
- (12) Lan, P.; Takahashi, E. J.; Liu, K.; Fu, Y.; Midorikawa, K. Carrier envelope phase dependence of electron localization in the multicycle regime. *New J. Phys.* **2013**, *15* (6), No. 063023.
- (13) Kremer, M.; Fischer, B.; Feuerstein, B.; de Jesus, V. L. B.; Sharma, V.; Hofrichter, C.; Rudenko, A.; Thumm, U.; Schröter, C. D.; Moshhammer, R.; Ullrich, J. Electron Localization in Molecular Fragmentation of H2 by Carrier-Envelope Phase Stabilized Laser Pulses. *Phys. Rev. Lett.* **2009**, *103* (21), 213003.
- (14) Jones, D. J.; Diddams, S. A.; Ranka, J. K.; Stentz, A.; Windeler, R. S.; Hall, J. L.; Cundiff, S. T. Carrier-Envelope Phase Control of Femtosecond Mode-Locked Lasers and Direct Optical Frequency Synthesis. *Science* **2000**, *288* (5466), 635–639.
- (15) Telle, H. R.; Steinmeyer, G.; Dunlop, A. E.; Stenger, J.; Sutter, D. H.; Keller, U. Carrier-envelope offset phase control: A novel concept for absolute optical frequency measurement and ultrashort pulse generation. *Appl. Phys. B: Laser Opt.* **1999**, *69* (4), 327–332.
- (16) Holzwarth, R.; Udem, T.; Hänsch, T. W.; Knight, J. C.; Wadsworth, W. J.; Russell, P. S. J. Optical Frequency Synthesizer for Precision Spectroscopy. *Phys. Rev. Lett.* **2000**, *85* (11), 2264–2267.
- (17) Wittmann, T.; Horvath, B.; Helml, W.; Schätzel, M. G.; Gu, X.; Cavalieri, A. L.; Paulus, G. G.; Kienberger, R. Single-shot carrier-envelope phase measurement of few-cycle laser pulses. *Nat. Phys.* **2009**, *5* (5), 357–362.
- (18) Sayler, A. M.; Rathje, T.; Müller, W.; Rühle, K.; Kienberger, R.; Paulus, G. G. Precise, real-time, every-single-shot, carrier-envelope phase measurement of ultrashort laser pulses. *Opt. Lett.* **2011**, *36* (1), 1–3.
- (19) Debrah, D. A.; Stewart, G. A.; Basnayake, G.; Tisch, J. W. G.; Lee, S. K.; Li, W. Direct in-situ single-shot measurements of the absolute carrier-envelope phases of ultrashort pulses. *Opt. Lett.* **2019**, *44* (14), 3582–3585.

- (20) Dietrich, P.; Krausz, F.; Corkum, P. B. Determining the absolute carrier phase of a few-cycle laser pulse. *Opt. Lett.* **2000**, *25* (1), 16–18.
- (21) Fukahori, S.; Ando, T.; Miura, S.; Kanya, R.; Yamanouchi, K.; Rathje, T.; Paulus, G. G. Determination of the absolute carrier-envelope phase by angle-resolved photoelectron spectra of Ar by intense circularly polarized few-cycle pulses. *Phys. Rev. A* **2017**, *95* (5), No. 053410.
- (22) Rathje, T.; Sayler, A. M.; Zeng, S.; Wustelt, P.; Figger, H.; Esry, B. D.; Paulus, G. G. Coherent Control at Its Most Fundamental: Carrier-Envelope-Phase-Dependent Electron Localization in Photo-dissociation of a H₂⁺ Molecular Ion Beam Target. *Phys. Rev. Lett.* **2013**, *111* (9), No. 093002.
- (23) Kling, M. F.; von den Hoff, P.; Znakovskaya, I.; de Vivie-Riedle, R. (Sub-)femtosecond control of molecular reactions via tailoring the electric field of light. *Phys. Chem. Chem. Phys.* **2013**, *15* (24), 9448–9467.
- (24) Kling, M. F.; Siedschlag, C.; Znakovskaya, I.; Verhoef, A. J.; Zherebtsov, S.; Krausz, F.; Lezius, M.; Vrakking, M. J. J. Strong-field control of electron localisation during molecular dissociation. *Mol. Phys.* **2008**, *106* (2–4), 455–465.
- (25) Li, H.; Tong, X. M.; Schirmel, N.; Urbasch, G.; Betsch, K. J.; Zherebtsov, S.; Süßmann, F.; Kessel, A.; Trushin, S. A.; Paulus, G. G.; Weitzel, K. M.; Kling, M. F. Intensity dependence of the dissociative ionization of DCl in few-cycle laser fields. *Journal of Physics B: Atomic, Molecular and Optical Physics* **2016**, *49* (1), No. 015601.
- (26) Li, H.; Kling, N. G.; Förg, B.; Stierle, J.; Kessel, A.; Trushin, S. A.; Kling, M. F.; Kaziannis, S. Carrier-envelope phase dependence of the directional fragmentation and hydrogen migration in toluene in few-cycle laser fields. *Struct. Dyn.* **2016**, *3* (4), No. 043206.
- (27) Basnayake, G.; Ranathunga, Y.; Lee, S. K.; Li, W. Three-dimensional (3D) velocity map imaging: from technique to application. *J. Phys. B-At. Mol. Opt. Phys.* **2022**, *55* (2), No. 023001.
- (28) Debrah, D. A.; Stewart, G. A.; Basnayake, G.; Nomerotski, A.; Svihra, P.; Lee, S. K.; Li, W. Developing a camera-based 3D momentum imaging system capable of 1 Mhits/s. *Rev. Sci. Instrum.* **2020**, *91* (2), No. 023316.
- (29) Lee, S. K.; Cudry, F.; Lin, Y. F.; Lingenfelter, S.; Winney, A. H.; Fan, L.; Li, W. Coincidence ion imaging with a fast frame camera. *Rev. Sci. Instrum.* **2014**, *85* (12), 123303.
- (30) Lee, S. K.; Lin, Y. F.; Lingenfelter, S.; Fan, L.; Winney, A. H.; Li, W. Communication: Time- and space-sliced velocity map electron imaging. *J. Chem. Phys.* **2014**, *141* (22), 221101.
- (31) Liao, Q.; Winney, A. H.; Lee, S. K.; Lin, Y. F.; Adhikari, P.; Li, W. Coulomb-repulsion-assisted double ionization from doubly excited states of argon. *Phys. Rev. A* **2017**, *96* (2), No. 023401.
- (32) Lin, Y. F.; Lee, S. K.; Adhikari, P.; Herath, T.; Lingenfelter, S.; Winney, A. H.; Li, W. Note: An improved 3D imaging system for electron-electron coincidence measurements. *Rev. Sci. Instrum.* **2015**, *86* (9), No. 096110.
- (33) Miranda, M.; Arnold, C. L.; Fordell, T.; Silva, F.; Alonso, B.; Weigand, R.; L'Huillier, A.; Crespo, H. Characterization of broadband few-cycle laser pulses with the d-scan technique. *Opt. Express* **2012**, *20* (17), 18732–18743.
- (34) Fan, L.; Lee, S. K.; Tu, Y.-J.; Mignolet, B.; Couch, D.; Dorney, K.; Nguyen, Q.; Wooldridge, L.; Murnane, M.; Remacle, F.; Bernhard Schlegel, H.; Li, W. A new electron-ion coincidence 3D momentum-imaging method and its application in probing strong field dynamics of 2-phenylethyl-N, N-dimethylamine. *J. Chem. Phys.* **2017**, *147* (1), No. 013920.
- (35) Ren, X.; Summers, A. M.; Raju, P. K.; Vajdi, A.; Makhija, V.; Fehrenbach, C. W.; Kling, N. G.; Betsch, K. J.; Wang, Z.; Kling, M. F.; Carnes, K. D.; Ben-Itzhak, I.; Trallero-Herrero, C.; Kumarappan, V. Single-shot carrier-envelope-phase tagging using an $f-2f$ interferometer and a phase meter: a comparison. *J. Opt.* **2017**, *19* (12), 124017.
- (36) Mehendale, M.; Mitchell, S. A.; Likforman, J. P.; Villeneuve, D. M.; Corkum, P. B. Method for single-shot measurement of the carrier envelope phase of a few-cycle laser pulse. *Opt. Lett.* **2000**, *25* (22), 1672–1674.
- (37) Kakehata, M.; Takada, H.; Kobayashi, Y.; Torizuka, K.; Fujihira, Y.; Homma, T.; Takahashi, H. Single-shot measurement of carrier-envelope phase changes by spectral interferometry. *Opt. Lett.* **2001**, *26* (18), 1436–1438.
- (38) Hoerner, P.; Schlegel, H. B. Angular Dependence of Strong Field Ionization of CH₃X (X = F, Cl, Br, or I) Using Time-Dependent Configuration Interaction with an Absorbing Potential. *J. Phys. Chem. A* **2017**, *121* (31), 5940–5946.
- (39) Wood, R. M.; Zheng, Q.; Edwards, A. K.; Mangan, M. A. Limitations of the axial recoil approximation in measurements of molecular dissociation. *Rev. Sci. Instrum.* **1997**, *68* (3), 1382–1386.
- (40) Hammerich, A. D.; Manthe, U.; Kosloff, R.; Meyer, H. D.; Cederbaum, L. S. Time-dependent photodissociation of methyl iodide with five active modes. *J. Chem. Phys.* **1994**, *101* (7), 5623–5646.